Canadian Conference - Pacific Conference on Earthquake Engineering 2023
Vancouver, British Columbia
June 25th – June 30th, 2023

Numerical Modelling of CLT Shear Walls with Hyperelastic Hold-Downs

Sinha Lamia Sultana[1], Yuxin Pan[2], Solomon Tesfamariam[2] and Thomas Tannert[4*]

[1]MSc alumni, School of Engineering, University of Northern British Columbia, Prince George, Canada
[2]Assistant Professor, Department of Civil and Environmental Engineering, The Hong Kong University of Science and Technology, Hong Kong, China
[3]Professor, School of Engineering, University of British Columbia Okanagan, Kelowna, Canada
[4]Professor, School of Engineering, University of Northern British Columbia, Prince George, Canada
[*]thomas.tannert@unbc.ca (Corresponding Author)

ABSTRACT

The provisions of CSA O86 (2019) for Cross-laminated Timber (CLT) shear walls recommend the design of non-dissipative hold-downs (HDs) with sufficient deformability to facilitate wall rocking. A hyperelastic HD system was proposed to satisfy these criteria. In this study, a numerical model was developed to capture the behaviour of CLT shear walls with the hyperelastic HD system using data from previous component level and full-scale shear testing. Calibration parameters were derived for the OpenSees *'Hysteretic'* material model for each HD configuration utilizing data from six tests on shear walls with un-coupled panels, and validated with the results from twelve additional tests on shear walls with coupled panels. The average differences between test and model for corner uplift, force at peak lateral displacement and energy dissipation were found to be 7%, 12% and 11%, respectively. The model can be used to predict the performance of untested shear wall configurations. Finally, a two-storey platform-type shear wall was designed and modelled applying the calibrated *Hysteretic* model for the HDs.

Keywords: Cross-laminated timber, experimental testing, OpenSees model, Hysteretic material.

INTRODUCTION

Background

The use of timber in tall building construction has been aided by the advancement of mass timber products such as CLT [1]. Tall wood buildings require adequately designed anchorages or HDs; however, conventional HDs used in light-frame wood buildings are often not suitable for tall buildings with CLT shear walls as lateral load resisting system [2].

When a CLT shear wall is subjected to lateral loads, the CLT panel behaves like a rigid body, and the deformations occur mainly due to the deformations of the connections [3]. Research has shown that either pure rocking or a combination of rocking and sliding are the preferable kinematic modes for platform-type shear walls under the action of seismic loads [4]. However, the 2019 edition of the Canadian Standard for Engineering Design in Wood, CSA O86 [5] recommends that rocking should be the predominant mode of failure and sliding should be restricted.

Additionally, CSA O86 now requires that HDs should be designed as a non-dissipative connection. While conventional HDs provide sufficient deformation to facilitate rocking but they do show yielding and energy dissipation. This poses a new challenge in designing CLT shear walls with HDs that can provide a good balance between deformability and non-dissipative criteria. Recent research efforts have not specifically attempted to address this issue; this prompts the need to explore innovative HD solutions. Materials which exhibit large elastic deformations can provide a potential solution to this challenge.

Hyperelastic hold-downs

To provide a solution that satisfies the CSA O86 provisions, experimental studies were conducted at the University of Northern British Columbia (UNBC) on a HD system that utilizes hyperelastic rubber pads [6-9], which is necessary to allow rocking motion of CLT panel. The behaviour of hyperelastic rubber material makes it a potentially good candidate for non-dissipative HD in CLT shear walls. The hyperelastic HDs were designed and tested to find a suitable solution that can act as a non-dissipative connection but possess sufficient deformation capacity to facilitate rocking.

The main components of the hyperelastic HDs include elastomeric bearing pads, steel plate and steel rod, see Figure 1. A rectangular slot with rounded corners was made in the face of the CLT panels to insert the elastomeric bearing pad and steel plate, and a circular hole was drilled in the cross-section of the panel to place the steel rod. Different configurations of the HD were studied by varying the width and thickness of the elastomeric bearing. Results from uniaxial testing on hyperelastic HDs and full-scale testing on shear walls consisting of hyperelastic HDs demonstrated that these sustained large loads along with exhibiting elastic and almost non-dissipative behavior.

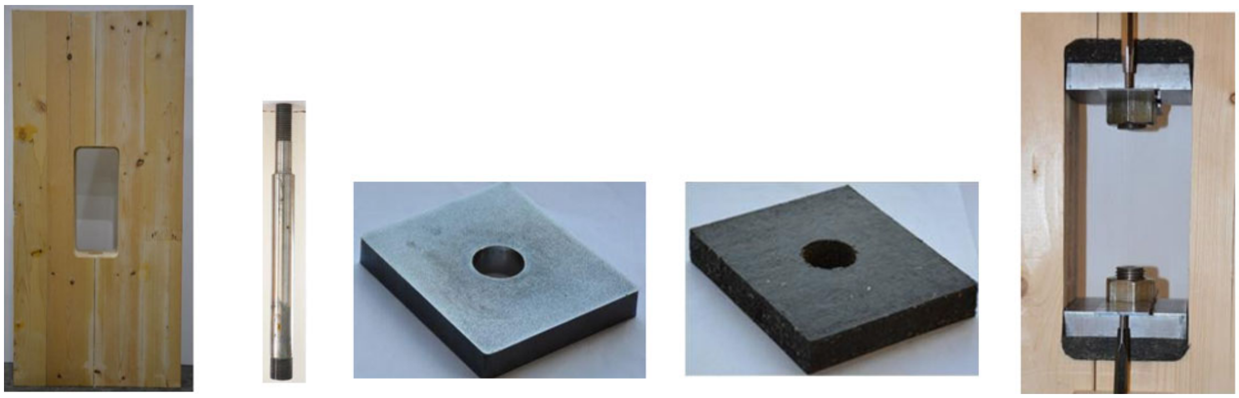

(a) (b) (c) (d) (e)

Figure 1. Details of HD assembly: (a) CLT panel, (b) steel rod, (c) steel pate, (d) elastomeric bearing, (e) HD.

Coupled shear walls with hyperelastic hold-downs

Full-scale tests were conducted for uncoupled and coupled CLT shear walls. All walls had aspect ratios of 3:1. The CLT was Grade VJ-1 5-ply, 139 mm thick, 3 m tall and 1.0 m wide, the spline was made up of D-fir 25×140×3000 mm surface mounted with 8×100 mm self-tapping screw (STS), and the HDs were made from Masticord elastomeric bearing pads, with widths 90 mm or 140 mm, and total thickness of 76, 102 or 127 mm (3, 4 or 5 inches. For coupled walls, the number of screws in the spline joint was varied. The HD configurations varied in terms of width and thickness of elastomeric bearing pad. The configurations of all tested walls are given in Table 1.

Table 1. Shear wall configurations with hyperelastic HDs

Configuration	HD thickness (mm)	HD width (mm)	No. of STS per side in spline
90-3-0	3	90	0
90-3-15	3	90	15
90-3-21	3	90	21
90-4-0	4	90	0
90-4-15	4	90	15
90-4-21	4	90	21
90-5-0	5	90	0
90-5-15	5	90	15
90-5-21	5	90	21
140-3-0	3	140	0
140-3-12	3	140	12
140-3-24	3	140	24
140-4-0	4	140	0
140-4-12	4	140	12
140-4-24	4	140	24
140-5-0	5	140	0
140-5-12	5	140	12
140-5-24	5	140	24

Shear keys with high horizontal stiffness were used to prevent sliding, one at the middle of each panel. The shear keys have elliptical holes that decouple shear resistance from uplift resistance. The shear key and spline are shown in Figure 2 (a) and (b).

Monotonic and cyclic tests were performed. The monotonic pushover tests were conducted at a rate of loading of 15mm/min until the wall resistance dropped to below 80% of the applied maximum force F_{max}. The reversed cyclic tests followed the abbreviated CUREE loading history [10], with a target displacement of 65% of the displacement achieved in the monotonic tests when the load dropped to 80% F_{max}. A typical coupled panel wall during testing is shown in Figure 2(c).

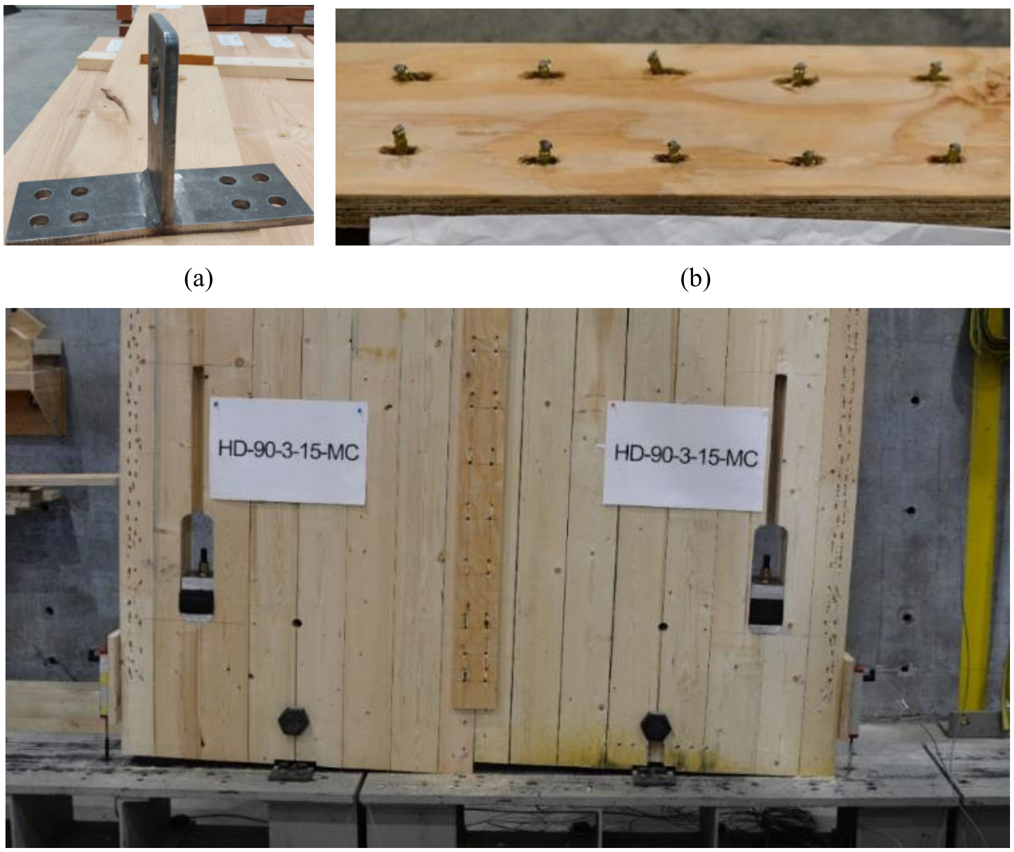

(a) (b)

(c)

Figure 2. Details of shear wall: (a) shear key, (b) spline joint, (c) typical coupled panel wall during testing.

The following trends were observed from the shear wall tests [9]: i) increasing the number of screws in the spline joint increased the peak forces and energy dissipation; ii) increasing the width of HD increased the stiffness of shear wall; and iii) increasing the thickness of the HD reduced the stiffness of shear wall. The trends in the effect of HD size on stiffness of shear wall agreed with the previous results of component level HD testing [6]. The energy dissipation in the shearwall was primarily occurring through the yielding of the spline joint, and the change in size of hyperelastic HD did not have much effect on energy dissipation of the shear wall.

Objectives

Numerical modelling saves time and cost invested in planning and performing large-scale experiments. Once a model is validated against experimental data, it can be utilized in studying various parameter combinations (such as aspect ratio of CLT panel, different types of connections, different types of ground motion, etc.) without extensive experimental research. Finding a suitable model for the hyperelastic HD can contribute to study the HD behaviour in several scenarios such as in a multi-storey shear wall or in a full-scale building.

The goal of this research was to investigate the performance of CLT shear walls with hyperelastic HDs through numerical modelling. The specific objectives were:

i) Develop a suitable model for the hyperelastic HDs;

ii) Validating models for CLT shear wall with hyperelastic HDs; and

iii) Model a two-storey platform-type shear wall with hyperelastic HDs.

MODELLING OF CLT SHEAR WALLS WITH HYPERELASTIC HOLD-DOWNS

Model development

The shear wall model was built in 2D in OpenSees [11]. The CLT panel and the shear keys were modelled as linear elastic elements, while the spline joint was modelled as non-linear energy dissipative element. The CLT panels were represented with shell elements while the connections were modelled as linear or non-linear springs as shown in Figure 3 (a).

The CLT was modelled using *Elastic Isotropic* material which belongs to the *nD material* class and represents "stress-strain relationships at the integration points of continuum and force-deformation elements" [12]. The material properties used for the CLT V2-1 grade were 9,500 MPa as Elastic Modulus (major strength axis) and 0.46 as Poisson's ratio [13]. The CLT panels were modelled using the *Quad* element, which generates four-node quadrilateral elements in 2D space. The material type was selected as "*PlaneStress*" and the *Elastic Isotropic* material was assigned.

The panel was meshed into smaller elements depending on the location of connections. Nodes were defined in accordance with the location of connection elements. These included the two HD elements, two shear key elements and four spline elements. The total strength of screws in spline was distributed into four elements, which is why there were four elements to represent the spline. This arrangement of nodes divided each CLT panel into ten smaller uniformly sized elements. It is worth mentioning that the CLT panel was meshed into even smaller elements during preliminary analysis; however, finer meshing was not producing any noteworthy change in the results and the deviation between test and model results was not affected.

The behavior of spline joints was represented by the Pinching4 material model. Two-node link elements with the calibrated Pinching4 material were placed in equal vertical intervals between the two CLT panels. The orientation of these elements was vertical. Horizontal zero-length springs, represented by elastic stiffness, were also assigned in the same locations to incorporate panel-to-panel friction in the vertical joint.

One shear key was placed at the middle of each panel. The shear key had a vertical pin that decoupled the vertical motion from the horizontal, to allow rocking behaviour. In absence of experimental data for load-displacement behaviour of shear key, a value for horizontal stiffness of 1,000 kN/mm was assumed for the shear key. The deformations recorded at the shear key locations during the shear wall testing were very small, and hence a high stiffness that would allow minimal sliding was assumed in the model. *Uniaxial Elastic* material was used to represent the load-displacement relationship and the shear keys were simulated as zero-length elements. Only horizontal zero-length elements were assigned, and no tension spring was assigned, as the shear key is free to move vertically.

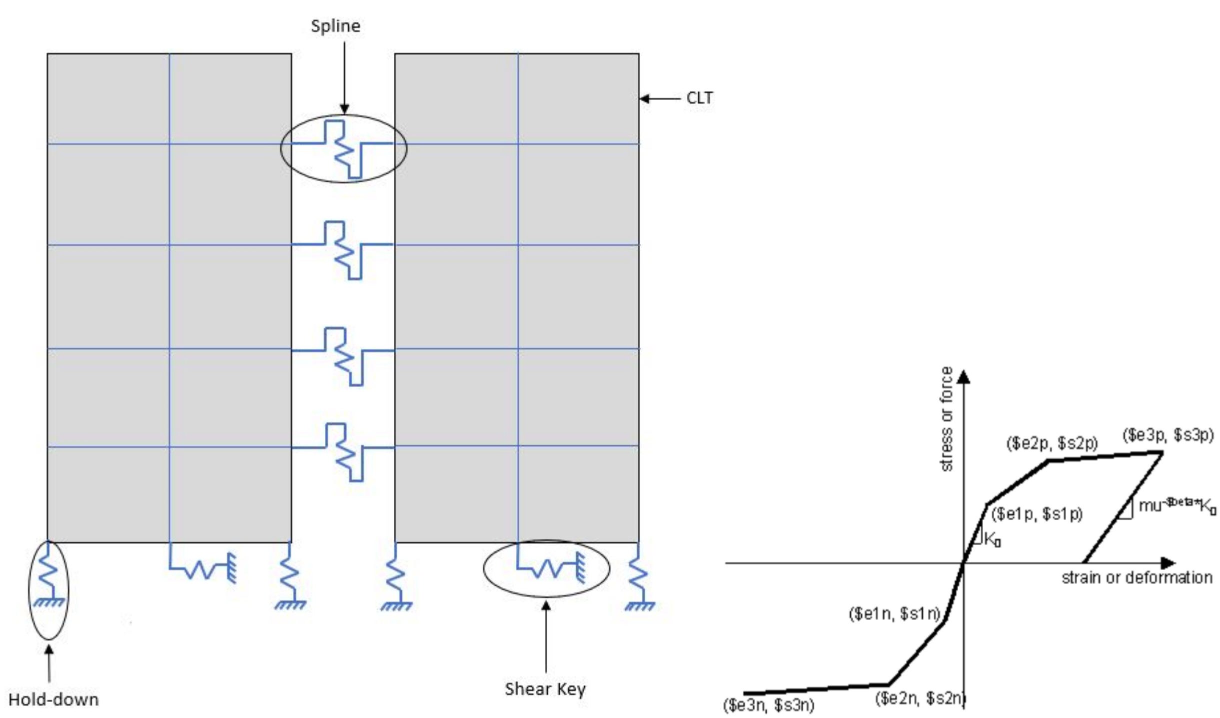

(a) *(b)*

Figure 3. Model: (a) schematic of a coupled shear wall model, (b) hysteretic model with parameters.

Previous studies on hyperelastic HDs showed their behaviour was almost non-dissipative, the load-deformation graph was nonlinear with stiffness increasing with larger displacements, and no residual deformation remained after the load was removed [6, 8]. Therefore, the HD was modelled with the uniaxial material model in the OpenSees library named *Hysteretic*. This material gives a bi-linear force deformation relationship which is defined using three sets of force-deformation points in the positive axes, three sets of force-deformation points in the negative axes, two pinching factors for defining pinching in stress and strain during reloading, two damage parameters for defining damage due to ductility or energy, and a factor for defining degraded unloading stiffness, as shown in Figure 3 (b). While the material model is simple to implement, the calibration approach used was different this time. Instead of calibrating with component-level test data, the Hysteretic material parameters were fitted in such a way that the shear wall results matched closely. In this manner, the HD material model parameters were in effect back-calibrated from the shear wall model analysis.

The bottom nodes at the supports were fixed in both horizontal and vertical directions. During the shear wall tests, a uniform gravity load of 2 kN/m was acting on the wall. Uniform loads can only be applied to the beam or column elements in OpenSees. For the CLT panels modelled as shell elements, the uniform load was converted into point loads and placed on the nodes. The total load was calculated and then distributed among the nodes at the top of the wall according to their tributary areas.

Model calibration

The spline joint was calibrated using data from test on spline arrangements with 8 screws on each panel side (i.e., total 16 screws). The load-displacement points for the Pinching4 model were derived from the backbone of the experimental graph. The connection was then modelled as a two-node link element with one free node and one fixed node. The damage type was set to "energy" and the damage parameters were adjusted until a good match was obtained between experimental and simulation results. The test and simulation results are shown in Figure 4 (a). The energy dissipated on the positive sides of the envelope curves (up to 42 mm) for model and test were 211 kN-mm and 203 kN-mm, respectively, with a percentage difference of 4%, allowing the model to be deemed adequate. Here, during the test the maximum strength was attained on the tension side at 40 mm while on the compression side it was attained at 20 mm. The non-symmetry between the tension and compression side observed in the spline test, was not observed to this extent later in the shear wall tests. A symmetric model for the spline was therefore considered more appropriate.

The first step in shear wall calibrations was to select 3 sets of trial points of the backbone curve, which are the 6 calibration parameters, for modelling the HD configuration 90-3. These calibration parameters were used to define the *Hysteretic* material, which now represented the HD in the shear wall model. The shear wall configuration 90-3-0 was used for the back calibration of the HD 90-3, because this was the configuration without a spline connection and the effect of the energy dissipative material was eliminated while calibrating the HD material model. Therefore, the only nonlinear component influencing the response of the model (stiffness of load-displacement graph) was the HD, while the CLT and shear keys remained linear elastic. The shear wall model was analyzed under cyclic loading protocol, and the results from the analysis were superimposed on the test results. The set of trial calibration parameters were modified each time and the analysis repeated, until a close match was found between the analysis and test results. Once a satisfactory fit was established, these 6 calibration parameters were tested by applying them on a shear wall model with the same HD but with screws in spline, that is, shear wall configurations 90-3-15 and 90-3-21. The chosen calibration parameters were able to reproduce the test results of these two shear walls in a satisfactory manner, as shown in Figure 4 (b), where the dashed red lines are the model.

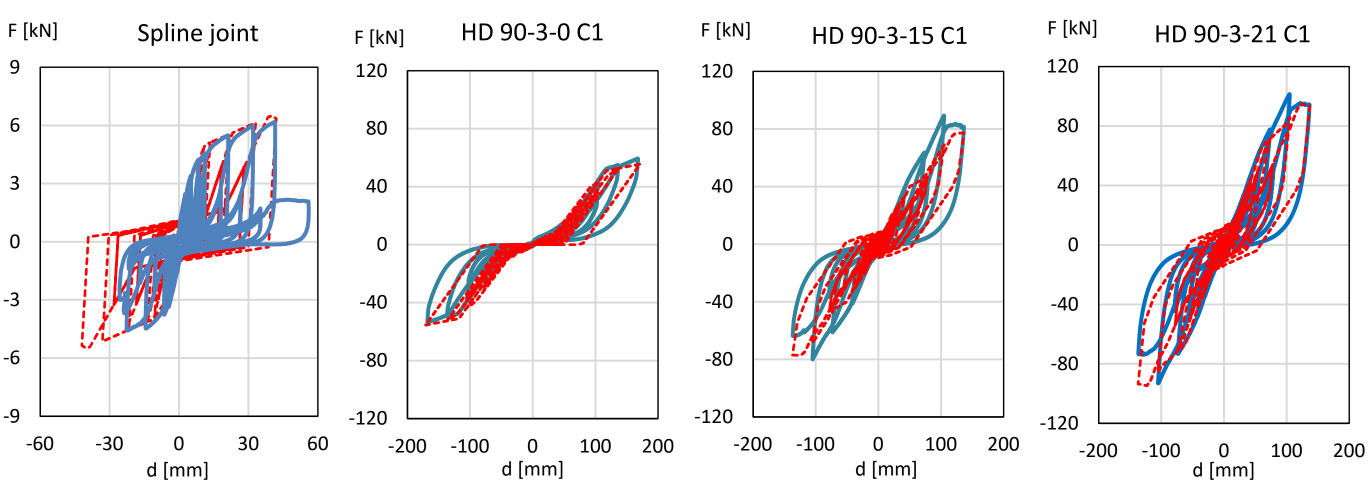

(a) *(b)* *(c)* *(d)*

Figure 4. Calibration of: (a) Pinching4 material for spline joint, (b) HD shear walls 90-3-0, (c) 90-3-15, (d) 90-3-21.

Shear wall results

The calibration model was adopted to model all 18 shear wall configurations (Table 1). The first set of trial calibration parameters for each HD configuration were selected based on judgement of how stiffness was expected to change with increase in HD thickness or width. For example, for the HD 90-4 the calibration parameters of HD 90-3 were used as the first trial set of points, and then fine-tuning was done with the awareness that the stiffness of this material will need to be reduced to calibrate it against shear wall 90-4-0. Similarly, for HD 140-3 the calibration parameters of HD 90-3 were taken and readjusted such that the stiffness of the material would increase. The results obtained from this calibration and subsequent shear wall model validation are presented in Figure 5 representative for all 140 mm wide HDs.

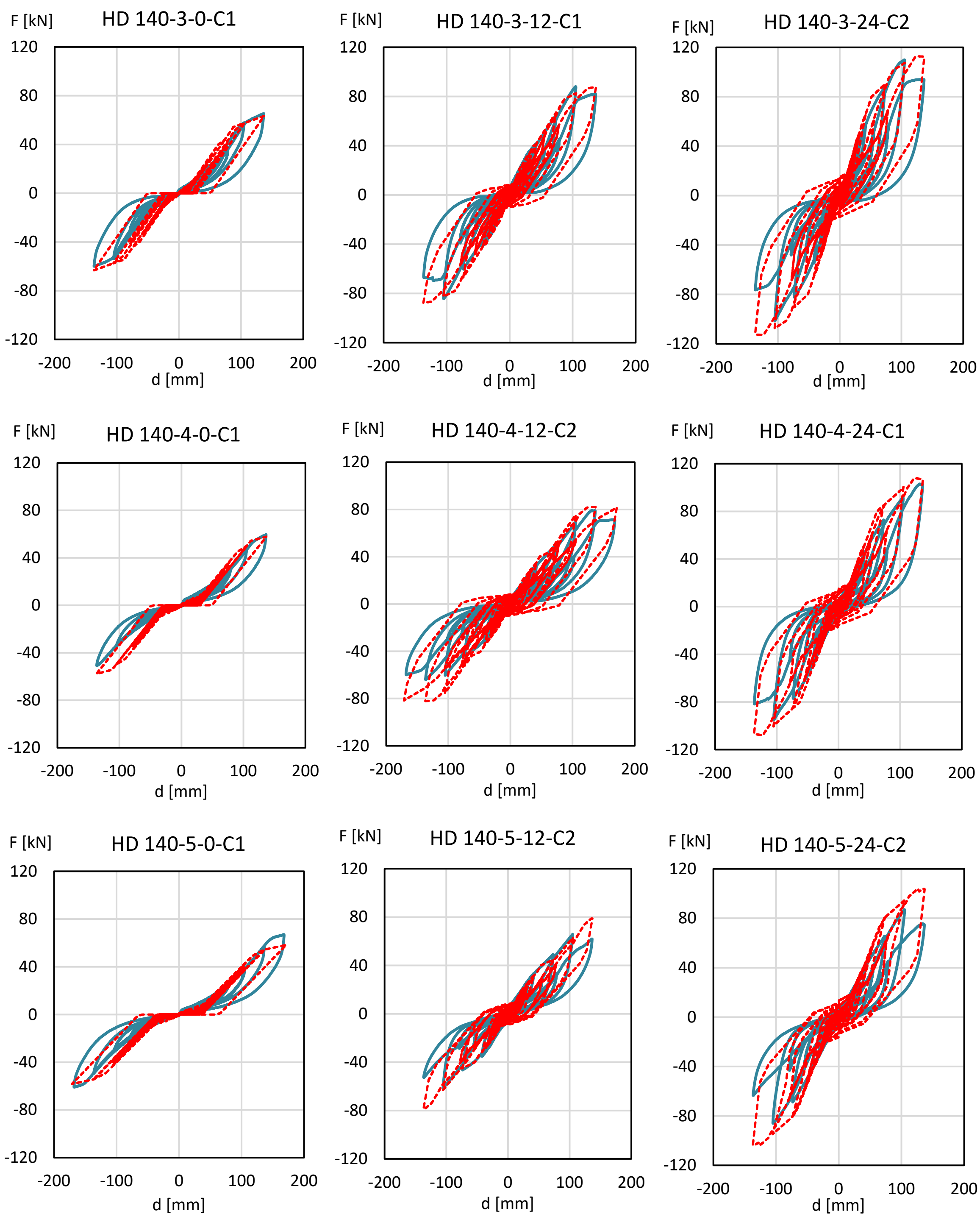

Figure 5. Modelled shear wall configurations with 140 mm wide HDs

Forces at peak lateral displacement, and dissipated energy

The forces at peak lateral displacement and the dissipated energy were calculated for all the shear wall configurations. The results are illustrated as bar plots for shear walls with 140 mm HDs in Figure 6. In the model it was observed that the uplifts were approximately one third of the peak lateral displacements, while the uplifts observed from test data were slightly lower, the average percentage difference being 7% between uplift values in test and model. The force at peak lateral displacements and energy dissipation increased as the number of screws increased in both test and model. The yield point was reached earlier (smaller displacement) for the stiffer HDs compared to the less stiff ones. This explains why the HDs in some shear walls yielded and contributed in energy dissipation, and in some others they did not. The average percentage difference between test and model for force at peak lateral displacement and energy dissipation were 12% and 11%, respectively.

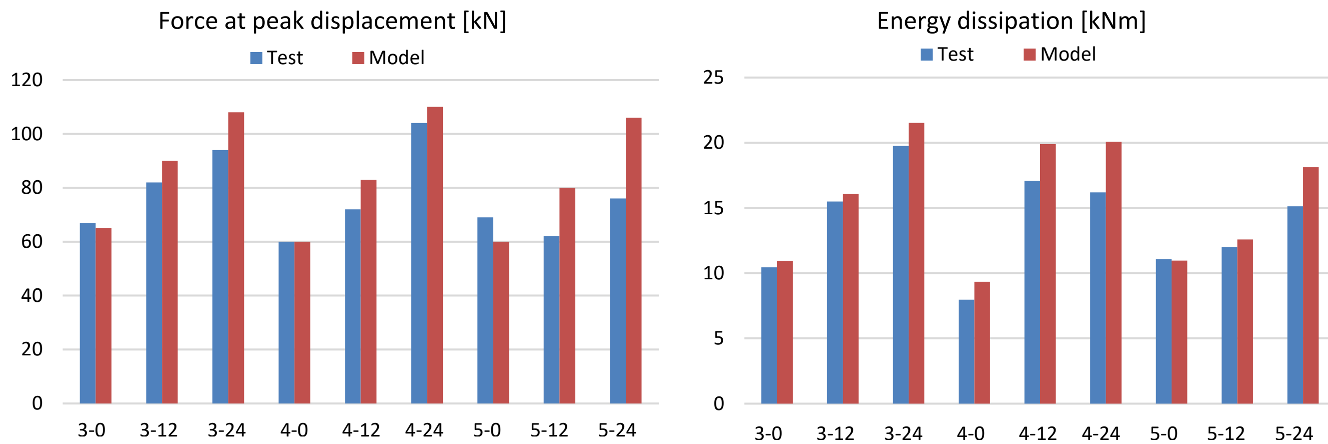

Figure 6. (a) Force at peak displacement, (b) energy dissipation for shear walls with 140 mm HDs

Calibration parameters for hyperelastic HDs

The set of calibration parameters obtained for each HD configuration are illustrated in Figure 7 (a), where, SF represents the shape factors of the elastomeric bearing. As the thickness of rubber layers increases, the SF decreases and so does the overall stiffness of the HDs. A set of equations was used to predict calibration parameters for untested HD configurations with 152, 178 and 203 mm (6, 7 and 8 inch) thick HDs, as illustrated in Figure 7 (b).

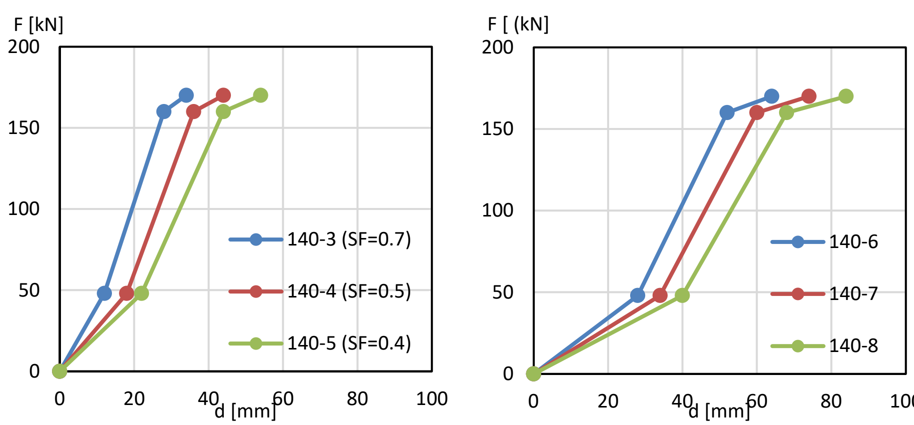

Figure 7. Graphical representation of calibration points of (a) tested configurations, (b) untested configurations

Two storey platform-type shear wall with hyperelastic HDs

A two-storey platform-type shear wall was designed with hyperelastic HDs using the same CLT material, spline joint and shear keys as in the previous tests. There was one HD and one shear key on each panel. The height and width of CLT panel were selected as 3m and 1.5m respectively. The strength and stiffness of connections were selected to resist a cumulative shear of 75 kN on the 1st storey and 50 kN on the 2nd storey, and a superimposed vertical dead load of 10 kN/m acting on each storey, see Figure 8 (a). For the 1st storey, the elastic strength and stiffness of spline were chosen as 90 kN and 36 kN/mm, respectively, and for the 2nd storey these values were 60 kN and 24 kN/mm, respectively. This was equivalent to 24 screws and 36 screws per panel side on the 1st and 2nd storey, respectively. Since the shear on the first storey was 1.5 times greater than that on the 2nd storey, the spline stiffness was selected to be 1.5 times greater for the 1st storey compared to the 2nd storey so that the spline yielding in both the stories would occur at the same time. The HD demands were found assuming coupled panel rocking behaviour. To select an appropriate HD configuration, the strength of the hyperelastic HDs were checked at the displacement which would give 1.5% inter-storey drift ratio (IDR), in this case 22.5 mm. The HDs were selected such that the strengths at 1.5% IDR (22.5mm displacement for HD) were greater than the demands on the HDs from the forces acting on the wall. Considering these, HDs 140-4 or 140-3 were the possible choices for the 1st storey and HDs of lower stiffness such as 140-6, 140-7 or 140-8 for the 2nd storey.

The two-storey shear wall was modelled in OpenSees as described previously. Floor nodes were added between 1st and 2nd storey, and on top of the 2nd storey, and the nodes were constrained with EqualDOF command. Inter-storey connections were added between the 1st and 2nd storey, and on the top of the 2nd storey. This shear wall model was analyzed under static monotonic pushover. A total monotonic displacement of 90 mm was applied to the top of the 2nd storey, equal to 1.5% IDR on each storey. From the analysis, it was observed that using HD 140-4 on 1st storey and HD 140-6 on the 2nd storey reached approximately equal inter-storey drifts; therefore, this was the final choice of HDs for each storey.

The results from the analysis are presented in Figure 8 (b). It can be observed that when the total displacement of 90 mm was reached, the wall attained a strength of 190 kN. The sum of responses of the shear keys on each storey shows the distribution of shear forces on that storey, which was 126 kN on the 2nd storey and 190 kN on the 1st storey. The spline on both storeys yielded at the same time and reached a maximum deformation of 17 mm. The inter-storey drift of 1st storey was 44 mm, while that of 2nd storey was 46 mm, equivalent to IDR of approximately 1.5% on each storey. The HDs on both storeys remained elastic and attained strengths close to the strengths that were predicted at 1.5% IDR. While the HD on 1st storey, HD 140-4, enters the zone where the stiffness increases, the HD on 2nd storey, HD 140-6, remained in the initial zone of low stiffness. According to the model predictions, both HDs will remain elastic until they attain a strength of 160 kN. The 1st storey HD will yield before the 2nd storey HD, when it reaches a deformation of 36 mm which is equivalent to inter-storey drift of 2.4% acting on the 1st storey. So, energy dissipation will occur through the spline only up to this point. If the number of screws in the spline were reduced, the demand on the HDs would increase and, in that case, stiffer HDs such as 140-3 or 140-2 might be required. Compared to HD 140-4, these stiffer HDs would yield earlier and start dissipating energy. Depending on the target performance for the HDs, the number of screws and HD configuration can be adjusted to obtain an optimum design.

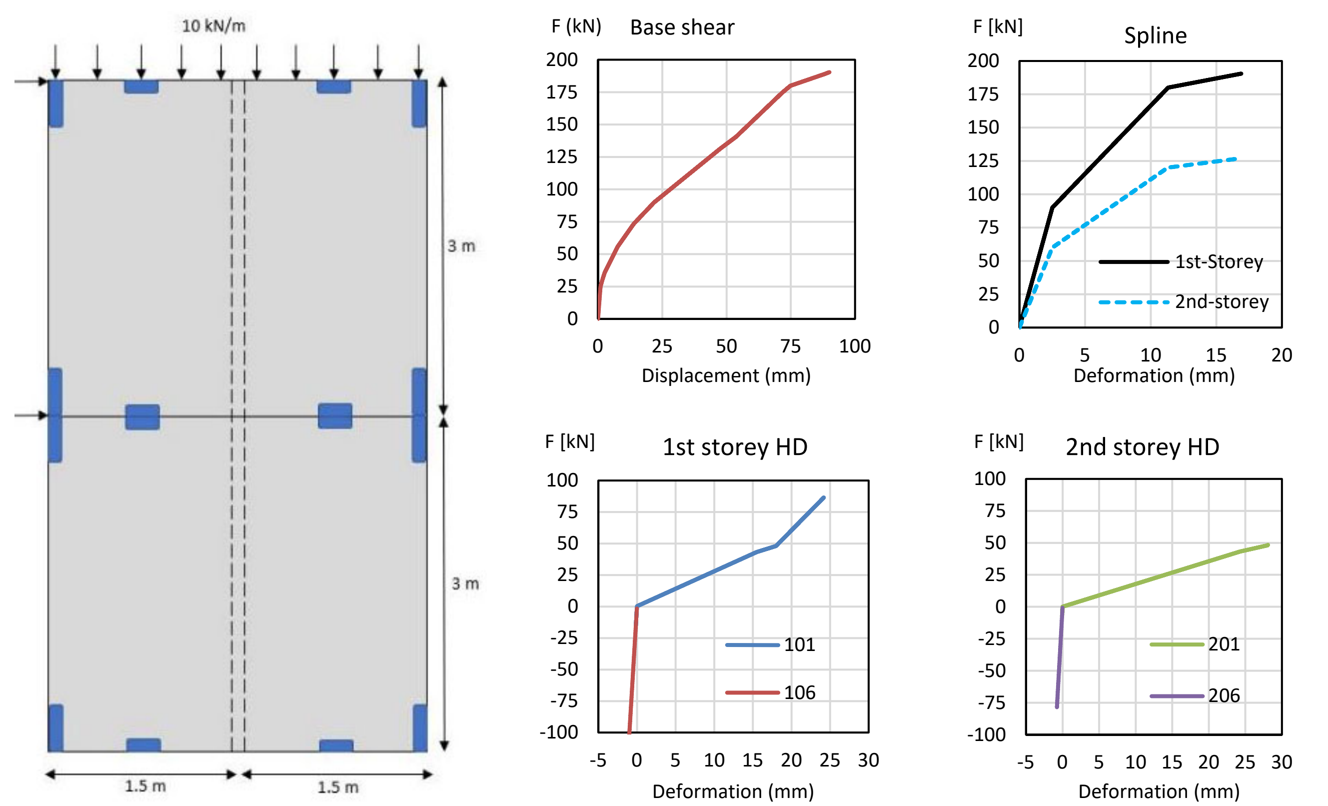

(a) (b)

Figure 8. Two storey platform-type shear wall (a) Model, (b) Results from static monotonic pushover analysis

CONCLUSIONS

A numerical model was developed to represent the novel hyperelastic HD system. The work can be summarized as follows:

i) To represent the hyperelastic HD behaviour, the back calibration method adopted with the *Hysteretic* material adequately predicted the corner uplift, force at peak lateral displacement and energy dissipation for the shear wall.

ii) Even though the HD component-level test data showed that the behaviour was hyperelastic with no stiffness degradation, this assumption was not valid when the HD performance was observed in the full-scale shear wall model. The HD stiffness adopted from the component level testing was leading to the overestimation of shear wall stiffness.

iii) The component level load-displacement data of hyperelastic HD tests represented the load-displacement behaviour of the elastomeric bearing under compression, without incorporating the effect of steel rod. As the steel rod yields after a certain load, reducing the HD stiffness provided a better fit for the global shear wall model.

iv) The parameters of the Hysteretic model were successfully calibrated as a function of rubber pad width and thickness. A set of equations was recommended to predict the calibration parameters of untested configurations of hyperelastic HDs. These parameters can be used for prediction of the load-displacement response of a new configuration of hyperelastic HD, and can be useful for both numerical modelling and prior to experimental testing.

v) The two-storey shear wall design can serve as a useful example to demonstrate how to select an appropriate hyperelastic HD for a given force and displacement demand. An optimum choice of HDs that gives equal inter-storey drifts on each storey can be achieved by utilizing the hyperelastic HD models.

ACKNOWLEDGMENTS

The research was funded by the Government of British Columbia through a BC Innovate Ignite grant, a Forest Innovation Investment Wood First grant, and a BC Leadership Chair. The support by the UNBC lab technicians James Andal, Michael Billups and Ryan Stern is greatly appreciated. Materials were provided by Structurlam Mass Timber Corporation (CLT) and JVI Inc. (elastomeric bearing pads).

REFERENCES

[1] Ceccotti A, Sandhaas C, Okabe M, Yasumura M, Minowa C, Kawai N. (2013). SOFIE project – 3D shaking table test on a seven-storey full-scale cross-laminated timber building. Eartquake Engineering and Structural Dynamics, 42:2003–2021.

[2] Tannert T, Loss C. (2022). Contemporary and novel hold-down solutions for mass timber shear walls. Buildings, 12(2), 202

[3] Poposvki M, Karacabeyli E. (2019). Chapter 4: Lateral design of cross-laminated timber buildings. In Karacabeyli & Gagnon (Eds.), CLT Handbook. Point-Claire, QC, Canada: FPInnovations.

[4] Izz, M, Casagrande D, Bezzi S, Pasca D, Follesa M, Tomasi R. (2018). Seismic behaviour of Cross-Laminated Timber structures: A state-of-the-art-review. Engineering Structures, 170, 42-52.

[5] CSA O86. Engineering Design in Wood (2019). Canadian Standards Association Standard O86 -. Mississauga, Ontario, Canada: CSA.

[6] Asgari H. (2020). Hyperelastic Hold-Down for Cross-Laminated Timber Shear Walls, MSc. Dissertation. University of Northern British Columbia, Prince George Canada.

[7] Oyawoye A A. (2021). High-capacity hyperelastic hold-down for cross-laminated timber shear walls, Project Report. University of Northern British Columbia, Prince George, Canada.

[8] Asgari H, Tannert T, Ebadi M, Loss C, Popovski M. (2021). Hyperelastic hold-down solution for CLT shear walls. Construction and Building Materials, 289, 123173.

[9] Tannert T, Oyawoye A A, Popovski M. (2022). Capacity-Based Design of CLT Shear Walls with Hyperelastic Hold Downs. International Network on Timber Engineering Research (INTER), Paper 55 - 15 – 4, Bad Aibling, Germany.

[10] ASTM E2126: Standard Test Methods for Cyclic (Reversed) Load Test. (2011) ASTM International, West Conshohocken.

[11] McKenna F, Fenves F, Mazzoni S, Scott M. (2006). OpenSees. Berkley, USA: University of California.

[12] Mazzoni S, McKenna F, Scott M H, Fenves G L. (2006). OpenSees Command Language Manual. Berkley, California: Pacific Earthquake Engineering Research Center.

[13] Crosslam CLT Technical Design Guide v4.0. (2018). Structurlam Penticton, British Columbia, Canada.